

## **Ternary transition metal chalcogenides with framework structures and the characterization of their bonding by magnetic properties**

Welf Bronger

Institut für Anorganische Chemie der Technischen Hochschule Aachen,  
Professor-Pirlet-Straße 1, D-5100 Aachen (F.R.G.)

**Abstract** - An extended Zintl principle is discussed for framework structures of ternary metal chalcogenides, pnictides and hydrides with tetrahedral and planar coordination of transition metal atoms. Their bonding can be characterized by the magnetic moments measured by susceptibilities and neutron diffraction. The experimental results are compared with crystal field splittings obtained by calculations based on the strong field model. This is an attempt to explain the occurrence of reduced spin states of transition metal atoms in tetrahedral coordination in terms of a dependence on the framework structure.

### INTRODUCTION

The subject matter of this report is the correlation between structure and bonding in ternary metal chalcogenides  $A_xM_yX_z$  where  $A \cong$  alkali metal,  $M \cong$  transition metal and  $X \cong$  sulfur or selenium. Not all the hitherto known compounds are to be included here; instead some selected examples will show which factors are significant for the formation of characteristic  $[M_yX_z]$  frameworks in the crystal structures and to what extent the complementary determination of magnetic moments by neutron diffraction allows insight into the characteristics of the chemical bond.

### SYNTHESIS OF TERNARY ALKALIMETAL - TRANSITION METAL CHALCOGENIDES

The first investigations on the existence of ternary sulfides of alkali metals and transition metals date back to about 1840 to 1875. Particularly noteworthy are the works of Völkner (ref. 1) and Schneider (ref. 2,3), from which it emerges that ternary sulfides are formed by fusing reactions of salts of the transition metals with sulfur and soda or potash. Some of these earlier findings were later confirmed around the turn of the century by Milbauer (ref. 4,5), who was able to synthesize ternary sulfides by reaction of KSCN with metal oxides at high temperatures. These older works then fell for a long time into oblivion, and it was not until the middle of the forties before new results were published by Rüdorff et al. (ref. 6-8), mainly on chromium and copper compounds. Interrelations in this field have now been recognized and are represented by a great number of new alkali metal-transition metal sulfides and selenides which have been characterized in recent times. Based on earlier findings on the preparation of ternary sulfides, methods have been developed for the isolation of pure substances. For this purpose hydrides or the metals themselves are used as alkali metal compounds besides the carbonates, sulfides or polysulfides. The reaction partners are then transition metals in elementary form and sulfur or hydrogen sulfide. For the syntheses of ternary selenides analogous methods have been developed. The reactions generally occur between 800 and 1200 °C in the melt, and on cooling under suitable conditions the ternary chalcogenides can be obtained as well formed, often beautifully coloured crystals.

In addition to the fusion reactions ternary chalcogenides can be prepared by intercalation of alkali metals in the layer structures of transition metal sulfides or selenides.

CHARACTERISTIC  $[M_yX_z]$  FRAMEWORKS IN THE CRYSTAL STRUCTURES OF TERNARY TRANSITION METAL CHALCOGENIDES

The crystal structures of the compounds  $A_xM_yX_z$  show the occurrence of characteristic  $[M_yX_z]$  frameworks (ref. 9,10). Table 1 contains some examples with  $M \cong \text{Mn, Fe or Co}$ , the crystal structures of which are characterized by  $MX_4$  tetrahedra mostly linked one- or two-dimensionally by their edges. In the iron sulfide with the highest alkali metal content,  $\text{Na}_5\text{FeS}_4$ ,

TABLE 1. Some ternary chalcogenides  $A_xM_yX_z$  with  $M \cong \text{Mn, Fe or Co}$

	$A_5\text{FeX}_4$ (ref. 13)	$A_6\text{CoX}_4$ (ref. 18)
	$A_3\text{FeX}_3$ (ref. 14,15)	
$A_2\text{MnX}_2$ (ref. 11)	$A\text{FeX}_2$ (ref. 16,17)	
$A_2\text{Mn}_3\text{X}_4$ (ref. 12)		$A_2\text{Co}_3\text{X}_4$ (ref. 12,19)

isolated  $[\text{FeS}_4]$  tetrahedra are separated by the alkali metal atoms. Fig. 1 shows the arrange-

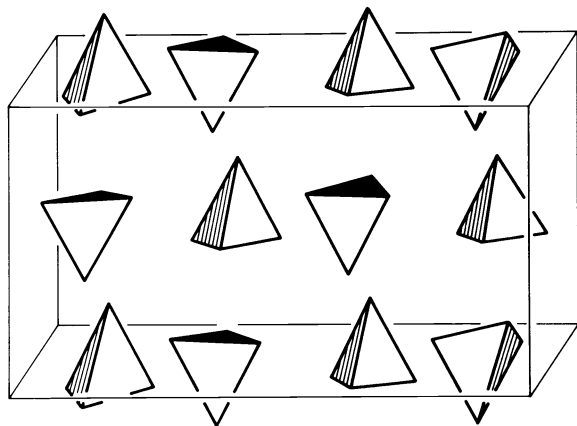


Fig. 1. The structure of  $\text{Na}_5\text{FeS}_4$ . Only the arrangement of the  $[\text{FeS}_4]$  tetrahedra is shown.

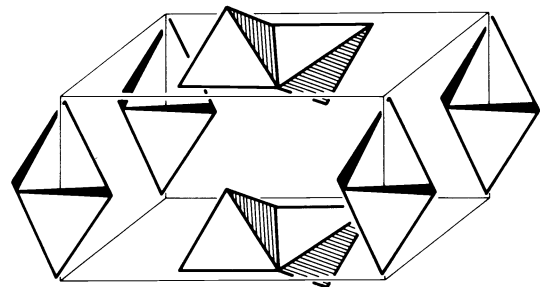


Fig. 2. The structure of  $\text{Na}_3\text{FeS}_3$ . Only the arrangement of the  $[\text{Fe}_2\text{S}_6]$  groups is shown.

ment of the tetrahedra, the positions of the alkali metal atoms being omitted for clearness. The structure of the ternary iron compounds  $\text{Na}_3\text{FeS}_3$  and  $\text{Na}_3\text{FeSe}_3$  is characterized by  $[\text{Fe}_2\text{X}_6]$  units (see Fig. 2), in which the two iron atoms are coordinated tetrahedrally by sulfur or selenium atoms. The two tetrahedra have one common edge. The alkali metal atoms form layers between these units. The framework structures of the compounds  $A\text{FeX}_2$  are built up by infinite chains in which the iron atoms again are coordinated tetrahedrally by chalcogen atoms. The chalcogen tetrahedra are linked onedimensionally by their edges. The alkali metal atoms have different coordination numbers according to their size. Fig. 3 shows the  $\text{KFeS}_2$ -type as an example. A similar chain structure type was found for the manganese chalco-

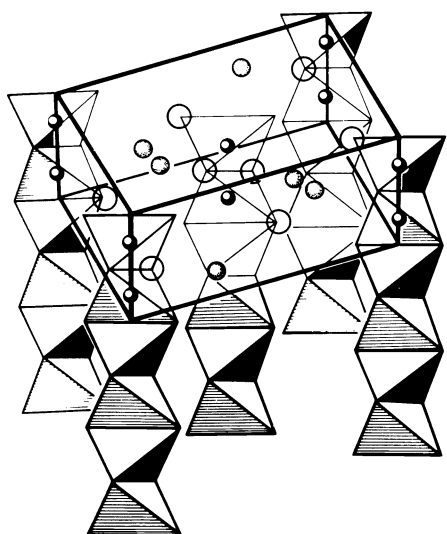


Fig. 3. The structure of  $\text{KFeS}_2$ . Open circles: X-, closed circles: M-, dotted circles: A-positions. These symbols are also used in the following figures.

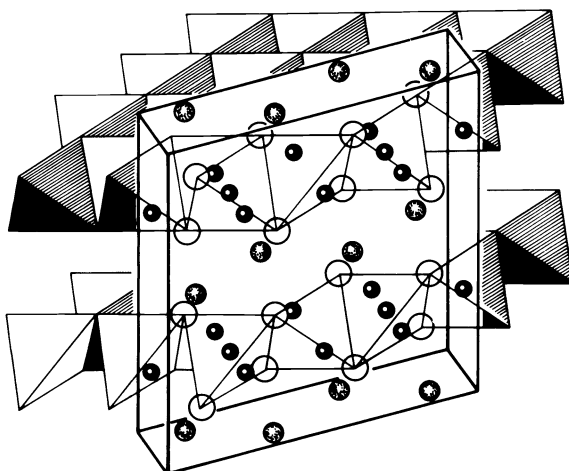


Fig. 4. The structure of  $\text{Cs}_2\text{Mn}_3\text{S}_4$

genides  $\text{A}_2\text{MnX}_2$ ; compounds of the stoichiometry  $\text{A}_2\text{Mn}_3\text{X}_4$  crystallize in a layer structure type (see Fig. 4). Here sulfur tetrahedra are linked again by edges, but now in a twodimensional arrangement. According to the stoichiometry in the  $[\text{Mn}_3\text{X}_4]$ -framework only three of four tetrahedral sites are occupied. The ternary cobalt chalcogenides  $\text{A}_2\text{Co}_3\text{X}_4$  are isostructural with

TABLE 2. Some ternary chalcogenides  $\text{A}_x\text{M}_y\text{X}_z$  with  $\text{M} \equiv \text{Ni, Pd or Pt}$

	$\text{A}_2\text{PdX}_2$ (ref. 21,22)	$\text{A}_2\text{PtX}_2$ (ref. 24)
$\text{A}_2\text{Ni}_3\text{X}_4$ (ref. 20)	$\text{A}_2\text{Pd}_3\text{X}_4$ (ref. 23)	$\text{A}_2\text{Pt}_3\text{X}_4$ (ref. 25)

the manganese compounds. With sodium a sulfide of the stoichiometry  $\text{A}_6\text{CoX}_4$  could be synthesized. The structure shows isolated  $[\text{CoS}_4]$ -Tetrahedra. Table 2 contains some ternary chalcogenides  $\text{A}_x\text{M}_y\text{X}_z$  with  $\text{M} \equiv \text{Ni, Pd or Pt}$ . Within the  $[\text{M}_y\text{X}_z]$ -frameworks the M atoms have again the coordination number Four but now they are surrounded by a planar arrangement of chalcogen atoms. The resulting rectangular arrays are linked one- or twodimensionally by their sides. Fig. 5 shows the  $\text{K}_2\text{PtS}_2$ -type as an example for a chain structure, Fig. 6 the  $\text{Cs}_2\text{Pd}_3\text{S}_4$ -type with a layerlike arrangement.

Regarding structural properties the preconditions here are similar to those in the case of Zintl phases, where elements on the borderline between metals and nonmetals are combined with a more electropositive partner, i.e. an alkali metal, in a binary compound. Analogous to these Zintl phases in the ternary chalcogenides under discussion anionic parts of the structure, in this case transition metal chalcogenide frameworks  $[\text{M}_y\text{X}_z]$ , can be obtained because the cationic partner again is an alkali metal. With the composition  $\text{A}_x[\text{M}_y\text{X}_z]$  a transfer of  $x$  electrons by means of alkali metal atoms yields an anion  $\text{M}_y\text{X}_z^{x-}$ . In accordance with the concept given by Zintl in a next step a prediction of the structure of this anion can be undertaken, for instance in comparison with the isoelectronic species  $\text{M}_y\text{Y}_z^{(x-z)-}$ , where the chalcogen X is replaced by a halogen Y. Thus the structure of  $\text{Fe}_2\text{S}_6^{6-}$  represented in Fig. 2 corresponds to the structure of  $\text{Fe}_2\text{Cl}_6$  in the same way as the  $\text{FeS}_4^{5-}$  or the  $\text{CoS}_4^{6-}$  anion correlate with the  $\text{FeCl}_4^-$  or the  $\text{CoCl}_4^{2-}$  anion respectively (Fig. 1), and the  $\text{PdS}_2^{2-}$  chain correlates with the chain in the structure of  $\text{PdCl}_2$  (Fig. 5). A corresponding replacement of the M atoms leads to equivalent predictions: Thus the framework structure of  $\text{FeS}_2^-$  corres-

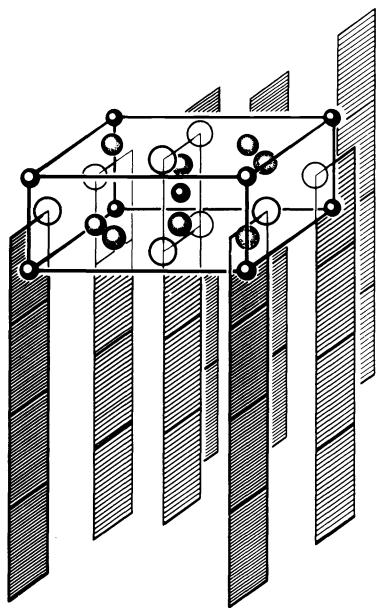


Fig. 5. The structure of  $K_2PtS_2$   
(left side)

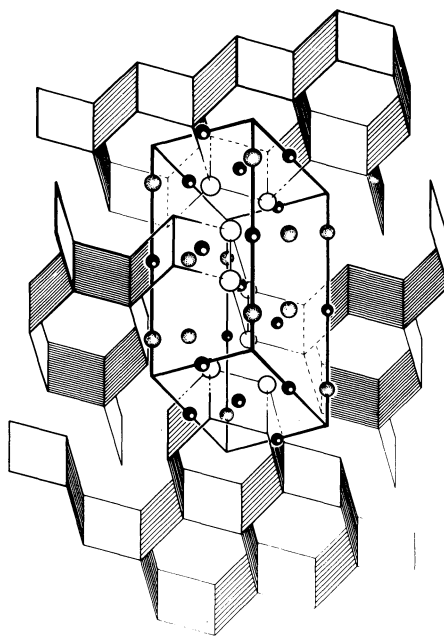


Fig. 6. The structure of  $Cs_2Pd_3S_4$   
(right side)

ponds to that of  $MnS_2^{2-}$ . In addition to and in accordance with the concept given the tabulated compounds show that an increase of the alkali metal content is connected with a dismantling of the framework structure as long as the oxidation number of M is not changed. Examples are shown by the following pairs:  $A_2Mn_3X_4 - A_2MnX_2$ ,  $AFeX_2 - A_3FeX_3$ ,  $A_3FeX_3 - A_5FeX_4$ ,  $A_2Co_3X_4 - A_6CoX_4$  or  $A_2Pd_3X_4 - A_2PdX_2$ . Frameworks consisting of smaller structural units occur chiefly with lighter alkali metals.

#### RELATIONSHIPS BETWEEN STRUCTURE AND MAGNETISM, AN INSIGHT INTO THE CHARACTERISTICS OF THE CHEMICAL BOND

Measurements of magnetic susceptibilities yielded the expected diamagnetism for planar coordinated  $d^8$ -transition metal atoms which are linked one- or twodimensionally within the framework structures of the palladates and platinates with the general compositions  $A_2MX_2$  and  $A_2M_3X_4$  (see Fig. 5 and 6). For the corresponding tetrahedrally coordinated  $d^5$ -transition metal atoms found within the framework structures  $AFeX_2$  and  $A_2Mn_3X_4$ , which are to be chosen as examples here, measurements of magnetic susceptibilities show a small, nearly temperature independent paramagnetism (ref. 16,26). This indicates antiferromagnetic coupling of the magnetic moments. Model calculations did not allow any conclusions on the size of the magnetic moments. However, investigations of series of mixed crystals,  $Cs_2(Zn_{1-\delta}Mn_\delta)_3S_4$  and  $CsGa_{1-\delta}Fe_\delta S_2$ , have provided further insight into this matter. In these series paramagnetic M atoms were gradually replaced by diamagnetic atoms of comparable size and the same oxidation number. In the first of the series mentioned above a magnetic moment of  $5.87 \mu_B$  for the manganese atoms was found for small manganese contents. When model calculations are used with additional consideration of antiferromagnetic interactions, this value of the magnetic moment also allows the interpretation of the temperature dependence of the susceptibility of mixed crystals with higher manganese contents (ref. 26). In contrast with what is observed in the Zn/Mn mixed crystals series, the M-S and M-M distances in the Ga/Fe series shorten significant with increasing iron content. Thus the magnetic moment changes and approaches the expected value for

a low spin state for the end composition  $\text{CsGa}_{0.55}\text{Fe}_{0.45}\text{S}_2$  (ref. 27).

As a check on the unusual finding of a low spin state of a tetrahedrally coordinated transition metal atom, neutron diffraction experiments were performed as a complementary investigation. These experiments allow the direct determination of magnetic moments at temperatures below the threedimensional ordering temperature. Powdered samples were measured using the BER II multicounter at the Hahn-Meitner Institut, Berlin. The diagrams obtained were evaluated with the aid of Rietveld's program for profile refinement (ref. 28). The results obtained for the chalcogenides  $\text{AFeX}_2$  with a  $[\text{FeX}_{4/2}]$  chain structure type are listed in TABLE 3. Fig. 7 presents the structures of the magnetic moments of the sulfides and the selenides.

TABLE 3. Crystallographic and magnetic data of some ternary compounds with chain structures

Compound	$\text{KFeS}_2$	$\text{KFeSe}_2$	$\text{RbFeS}_2$	$\text{RbFeSe}_2$
Average M-X distances (pm)	223.6	236.1	224.2	236.4
No. of nearest neighbours M and their distance to the central M atom (pm)	2x270.2	2x281.0	2x272.0	2x283.3
Néel temperature (K)	250(1)	310(1)	188(1)	249(1)
Neutron diffraction experiment T (K)	11	15	11	14
R value	0.056	0.070	0.065	0.043
Magnetic moment ( $\mu_B$ ) according to $\mu = 2\{S(S+1)\}^{1/2} \mu_B$	2.7(3)	4.2(3)	2.6(3)	3.5(1)
Magnetic space group	$\text{C2}'/\text{c}$	$\text{C2}/\text{c}'$	$\text{C2}'/\text{c}$	$\text{C2}/\text{c}'$

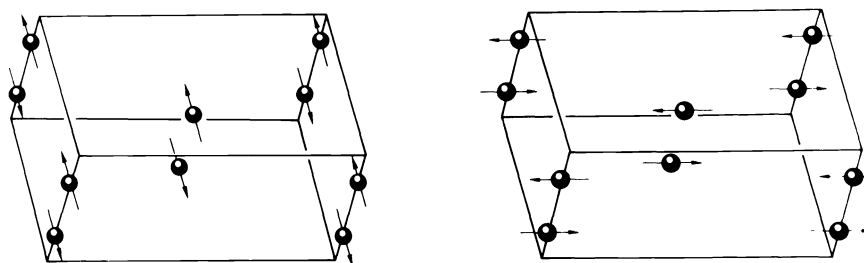


Fig. 7. The arrangements of the magnetic moments for  $\text{AFeS}_2$  (left side) and for  $\text{AFeSe}_2$  (right side)

In order to understand the size of the magnetic moments deviating from the value expected for  $d^5$  iron ions coordinated tetrahedrally by sulfur or selenium atoms in a chain structure the influence of the nearest neighbours on the electronic structure of the iron atoms was determined by means of model calculations. We started by applying the strong field method, neglecting interelectronic interactions and spin-orbit coupling. Since the five d electrons are supposed to move independently of one another under the influence of the ligands it is permissible to use the one-electron scheme as a starting point. On this basis the crystal field splitting of the fivefold degenerate orbital states can be calculated using the operator  $\hat{H}_1 = \hat{H}_0 + \hat{V}(r)$  where  $\hat{H}_0$  represents the operator of the undisturbed transition metal atom

and  $\hat{V}(r)$  is the perturbation by the environment. If  $\hat{H}_1$  operates on the real d orbitals as the basic set, the energy changes  $\Delta E$  prove to be approximately the roots of a  $5 \times 5$  secular determinant according to perturbation theory (ref. 29). In our calculations the ratio of the radial integral  $\langle r^2 \rangle$  to the radial integral  $\langle r^4 \rangle$  was chosen in such a way that the ratio  $\alpha_2/\alpha_4$  as defined by Companion and Komarynsky (ref. 30) became 3 for one ligand in the  $\text{FeS}_4^{5-}$  tetrahedron in  $\text{KFeS}_2$ . If the charges of the atoms are set equal to their oxidation numbers, the energy splittings can be calculated by means of a relative standard. The four chalcogen atoms and the nearest transition metal ions are taken as ligands; their distances are listed in TABLE 3. Supplementary calculations show that the influence of atoms at a greater distance can be neglected.

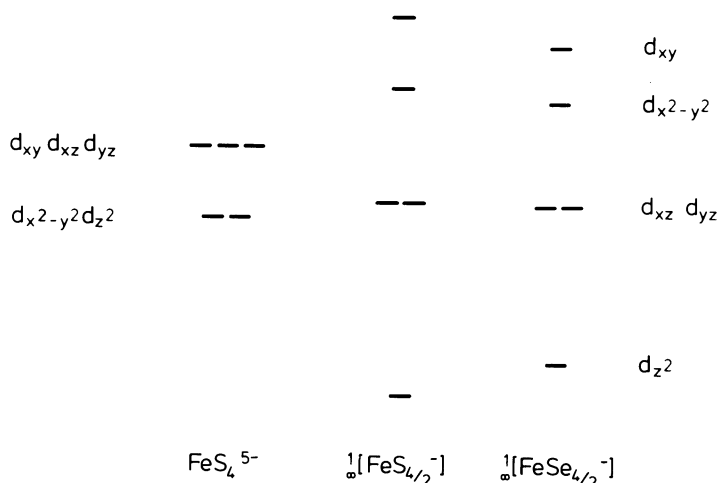


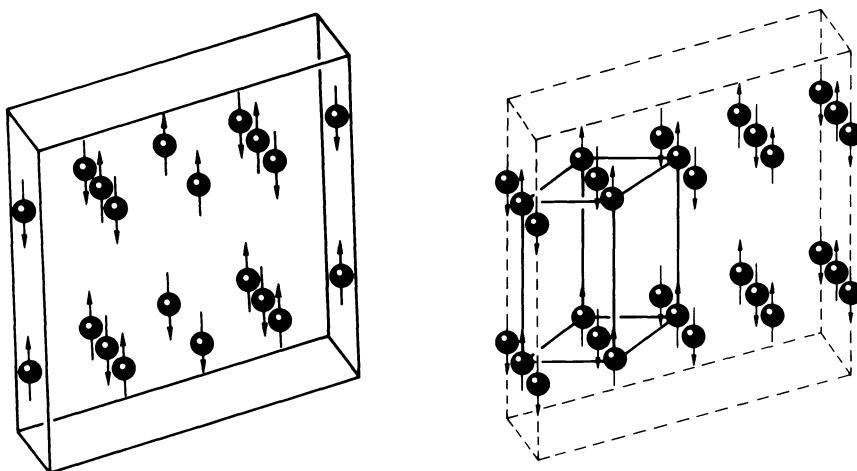
Fig. 8. Relative crystal field splittings calculated for some ternary iron chalcogenides

Fig. 8 shows the relative energy splittings correlated with an isolated  $[\text{FeS}_4]^{5-}$  tetrahedron and the chain structures of linked tetrahedra. The sequence of the measured magnetic moments (TABLE 3) reveals the expected correlation with the splittings. Thus the larger splittings and the smaller magnetic moments are found for the iron sulfides and the smaller splittings and the higher magnetic moments are found for the iron selenides. For the compound  $\text{Na}_5\text{FeS}_4$  a high spin state is expected, measurements are in preparation.

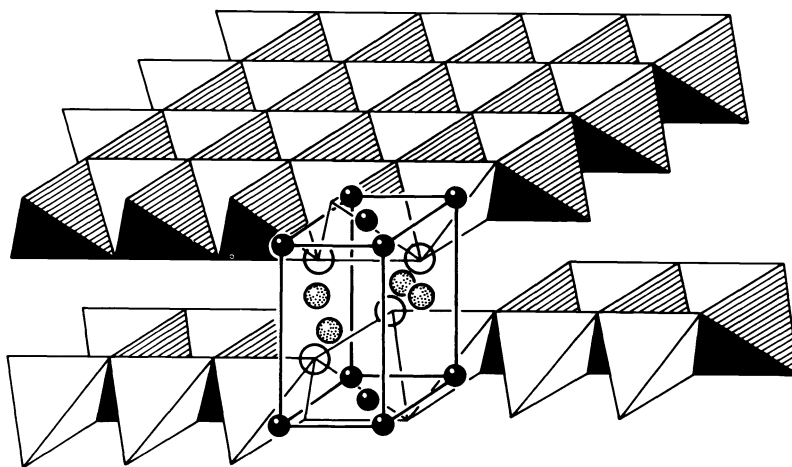
The simple model is able to predict the size of magnetic moments of ternary manganese compounds. In accordance with smaller energy splittings higher magnetic moments are expected. The experiments confirm this prediction (TABLE 4). Fig. 9 presents the structures of the magnetic moments of the compounds listed in TABLE 4. The structure of the above mentioned sulfide  $\text{Cs}_2\text{Mn}_3\text{S}_4$  is characterized by a framework in which sulfur tetrahedra are linked by edges in a two-dimensional arrangement. The manganese atoms occupy three of four tetrahedral sites (see Fig. 4). Mainly the larger M-S and M-M distances in comparison with the iron compounds  $\text{AFeS}_2$  (see TABLE 3) and the lower oxidation number of the M atoms yield a smaller crystal field splitting in the case of the manganese compound  $\text{Cs}_2\text{Mn}_3\text{S}_4$ . In accordance with this calculation a higher magnetic moment was found which is not far away from the value expected for a high spin state. The results of investigations on the compounds  $\text{NaMnP}$  and  $\text{NaMnAs}$  (ref. 31,32), also listed in TABLE 4, are in agreement with a further extension of

TABLE 4. Crystallographic and magnetic data of some ternary compounds with layer structures

Compound	$\text{Cs}_2\text{Mn}_3\text{S}_4$	$\text{NaMnP}$	$\text{NaMnAs}$
Average M-X distances (pm)	244	248.2	258.6
No. of nearest neighbours M and their distance to the central M atom (pm)	2x310 Mn(4b) 2x301 Mn(8g) 1x310	4x288.5	4x297.0
Néel temperature (K)	160(10)	560(10)	500(10)
Neutron diffraction experiment T (K)	4.2	15	13
R value	0.027	0.023	0.01
Magnetic moment ( $\mu_B$ ) according to $\mu = 2\{S(S+1)\}^{1/2} \mu_B$	5.0(1) Mn(4b) 4.7(1) Mn(8g)	4.5(1)	5.0(1)
Magnetic space group	$Ibam'$	$P4/n'm'm'$	$P4/n'm'm'$

Fig. 9. The arrangements of the magnetic moments for  $\text{A}_2\text{Mn}_3\text{S}_4$  (left side) and for  $\text{AMnP}$  and  $\text{AMnAs}$ , respectively (right side)

our model calculations to ternary phosphides and arsenides. Both compounds crystallize in a framework structure type similar to that of the ternary manganese sulfide (Fig.10). For  $\text{NaMnP}$  larger energy splittings in comparison with the sulfide  $\text{Cs}_2\text{Mn}_3\text{S}_4$  are calculated mainly

Fig. 10. The structure of  $\text{AMnP}$

because of the higher point charges substituting the phosphorus ligands. In accordance with the assumption of a higher charge on the phosphorus atoms compared with the sulfur atoms a smaller magnetic moment was found. For the arsenide again a larger magnetic moment was observed. The decrease of the energy splittings depends here on the increase of the M-X distances.

#### EXTENSION AND OUTLOOK

The ternary chalcogenides  $A_xM_yX_z$  described so far are in most cases compounds with 3d-transition metals. Chalcogenides with  $M \cong 4d$ - or  $5d$ -transition metal are hardly known. Only some palladium and platinum compounds, some intercalation phases in which alkali metals are intercalated in  $MX_2$  layer structures and some molybdenum and rhenium compounds have been discovered. In the systems A/Mo/X and A/Re/X ternary chalcogenides could be synthesized which con-

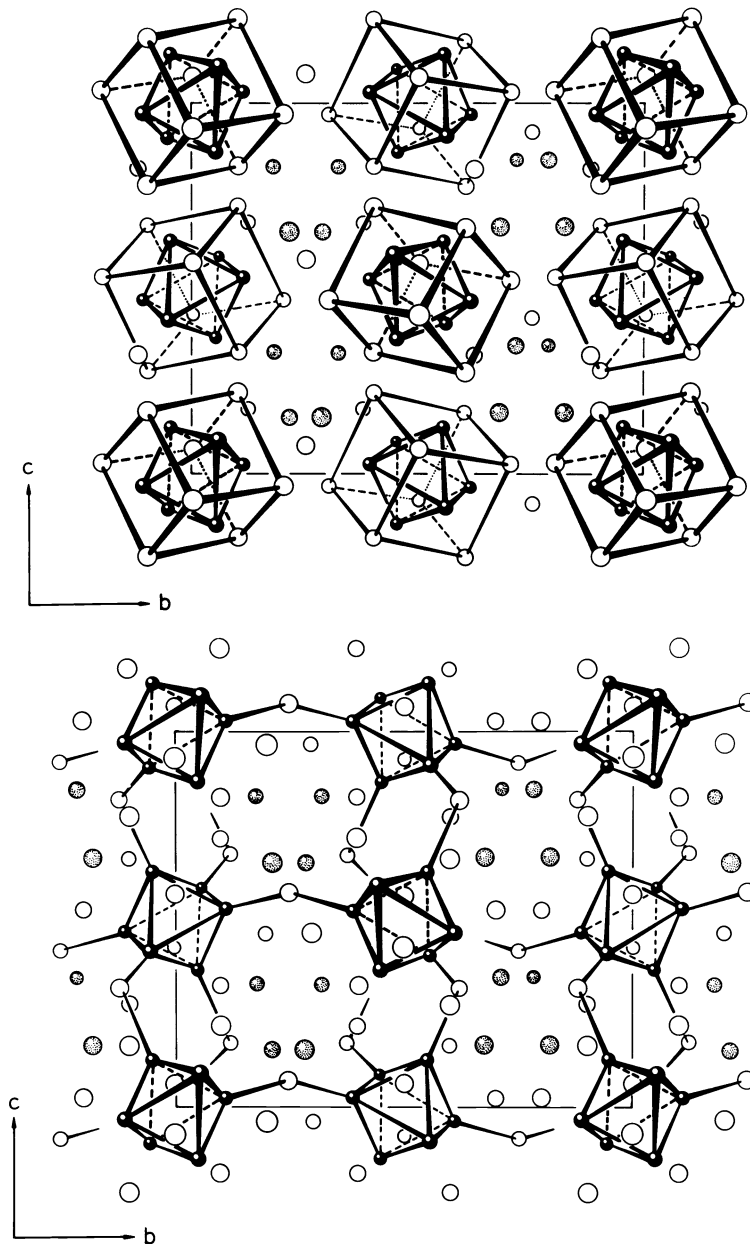


Fig.11. The structure of  $Li_4Re_6S_{11}$ . At the top the arrangement of the  $[Re_6S_8]$  clusters, at the bottom the linkage of the  $Re_6$ -units by sulfur atoms

tain isolated or condensed  $[M_6X_8]$  clusters as characteristic units of a framework structure. In accordance with the extension of Zintl's principle here again analogous atomic arrangements can be observed in binary systems  $M_Y Z$  where Y means a halogen. For example: In the system Li/Re/S the compound  $Li_4Re_6S_{11}$  was synthesized recently (ref. 33). Structure investigations show a framework in which isolated  $[Re_6S_8]$  clusters are linked three-dimensionally by additional sulfur atoms according to the scheme  $[Re_6S_8]S_{6/2}^{4-}$  (Fig. 11). The arrangement is analogous to that in  $Nb_6I_{11}$  or  $[Nb_6I_8]I_{6/2}$  (ref. 34,35). For this arrangement a most stable electronic configuration is obtained if 24 electrons for the 12 metal-metal-bondings in a  $M_6$ -unit are available. The  $Re_6$ -unit has this configuration while the  $Nb_6$ -unit has only 19 electrons. Therefore the rhenium compound is diamagnetic and the niobium compound paramagnetic. In the first one the  $M_6$ -octahedra are nearly regular, in the latter they are distorted according to a cooperative Jahn-Teller effect. This example shows that a framework structure can be preserved even if a system with more covalent bonding is shifted towards more electron-deficient bonding. This is well known from the so called intercalation compounds.

The before mentioned extension from the ternary chalcogenides to the corresponding phosphides and arsenides led to another group of ternary compounds, namely the ternary hydrides of the general composition  $A_x M_Y H_z$ . Here the transfer of x electrons by means of alkali metal

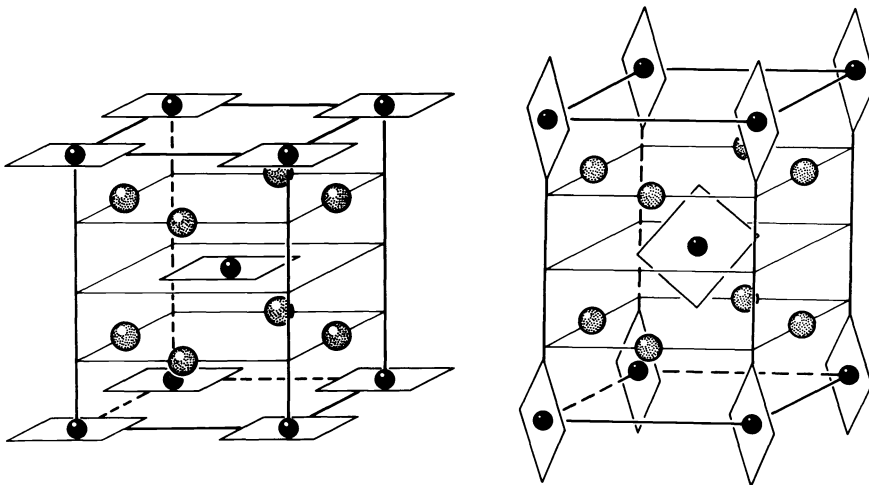


Fig. 12. The structure of  $Na_2PtH_4$  (left side) and the low-temperature structure of  $K_2PtH_4$  (right side)

atoms yields negatively charged hydrogen ligands building up anions  $M_Y H_z^{x-}$  direct comparable with halogenid anions  $M_Y Z^{x-}$ . Figure 12 shows the structures of the two hydrides  $Na_2PtH_4$  and  $K_2PtH_4$  (ref. 36,37). The isolated planar  $PtH_4^{2-}$ -units correspond to the  $PtCl_4^{2-}$ -group well known from the  $K_2PtCl_4$  structure type. A detailed report about such compounds is another story.

#### ACKNOWLEDGMENTS

The author wishes to thank the Bundesminister für Forschung und Technologie, the Deutsche Forschungsgemeinschaft and the Fonds der Chemischen Industrie for financial support.

## REFERENCES

1. A. Völker, Justus Liebig's Ann., **59**, 35-40 (1846).
2. R. Schneider, Poggendorffs Ann. Phys. Chem., **151**, 437-450 (1874).
3. R. Schneider, Ann. Physik., **136**, 460-467 (1869).
4. J. Milbauer, Z. Anorg. Allg. Chem., **42**, 333-449 (1904).
5. J. Milbauer, Z. Anorg. Allg. Chem., **42**, 450-452 (1904).
6. W. Rüdorff and K. Stegemann, Z. Anorg. Allg. Chem., **251**, 376-395 (1943).
7. W. Rüdorff, W.R. Ruston and A. Scherhauser, Acta Crystallogr., **1**, 196-200 (1948).
8. W. Rüdorff, H.G. Schwarz and M. Walter, Z. Anorg. Allg. Chem., **269**, 141-152 (1952).
9. W. Bronger, Angew. Chem., Int. Edn. Engl., **20**, 52-62 (1981).
10. W. Bronger and P. Müller, J. Less-Common Met., **100**, 241-247 (1984).
11. W. Bronger, D. Schmitz et al., unpublished.
12. W. Bronger and P. Böttcher, Z. Anorg. Allg. Chem., **390**, 1-12 (1972).
13. K. Klepp and W. Bronger, Z. Anorg. Allg. Chem., in press.
14. P. Müller and W. Bronger, Z. Naturforsch., **34b**, 1264-1266 (1979).
15. P. Müller and W. Bronger, Z. Naturforsch., **36b**, 646-648 (1981).
16. W. Bronger, Z. Anorg. Allg. Chem., **359**, 225-233 (1968).
17. H. Boller and H. Blaha, Monatsh. Ch., **114**, 145-154 (1983).
18. K. Klepp and W. Bronger, Z. Naturforsch., **38b**, 12-15 (1983).
19. W. Bronger, P. Böttcher and U. Hendriks, unpublished.
20. W. Bronger, J. Eyck, W. Rüdorff and A. Stössel, Z. Anorg. Allg. Chem., **375**, 1-7 (1970).
21. W. Bronger, O. Günther, J. Huster and M. Spangenberg, J. Less-Common Met., **50**, 49-55 (1976).
22. W. Bronger, D. Schmitz and R. Rennau, unpublished.
23. J. Huster and W. Bronger, J. Solid State Chem., **11**, 254-260 (1974).
24. W. Bronger and O. Günther, J. Less-Common Met., **27**, 73-79 (1972).
25. O. Günther and W. Bronger, J. Less-Common Met., **31**, 255-262 (1973).
26. W. Bronger, P. Müller and U. Hendriks, unpublished.
27. W. Bronger and P. Müller, J. Less-Common Met., **70**, 253-262 (1980).
28. H.M. Rietveld, J. Appl. Crystallogr., **2**, 65-71 (1969).
29. H.L. Schläfer and G. Gliemann, Einführung in die Ligandenfeldtheorie, Akademie Verlagsgesellschaft, Frankfurt (1967).
30. A.L. Companion and M.A. Komarynsky, J. Chem. Educ. **41**, 257-262 (1964).
31. G. Achenbach and H.-U. Schuster, Z. Anorg. Allg. Chem., **475**, 9-17 (1981).
32. L. Linowsky and W. Bronger, Z. Anorg. Allg. Chem., **409**, 221-227 (1974).
33. W. Bronger, H.-J. Miessen, P. Müller and R. Neugröschel, J. Less-Common Met., in press.
34. L.R. Bateman, J.F. Blount and L.F. Dahl, J. Am. Chem. Soc., **88**, 1082-1085 (1966).
35. A. Simon, H.-G. von Schnering and H. Schäfer, Z. Anorg. Allg. Chem., **355**, 295-310 (1967).
36. W. Bronger, P. Müller, D. Schmitz and H. Spittank, Z. Anorg. Allg. Chem., **516**, 35-41 (1984).
37. W. Bronger, P. Müller and G. Auffermann, unpublished.